PHYSICAL REVIEW B **80**, 161404(R) (2009)

Atomic configurations and energetics of vacancies in hexagonal boron nitride: First-principles total-energy calculations

Susumu Okada

Graduate School of Pure and Applied Sciences and Center for Computational Sciences, University of Tsukuba, 1-1-1 Tennodai, Tsukuba 305-8571, Japan

and CREST, Japan Science and Technology Agency, 4-1-8 Honcho, Kawaguchi, Saitama 332-0012, Japan

(Received 10 August 2009; published 12 October 2009)

We investigate the energetics and electronic structure of multiatomic vacancies in hexagonal boron nitride (*h*-BN) based on the local-density approximation in the density-functional theory. We find that the energetics of vacancies strongly depends not only on the environmental condition of boron and nitrogen chemical potentials but also on electron chemical potentials of these systems. Under nitrogen- and electron-rich conditions, the triangular vacancy comprised of one nitrogen and three boron atoms is a geometrically favorable structure. We also find that the atomic structure of vacancies depends on their charge state. In vacancies with nitrogen edges, the distance between the next-nearest-neighbor nitrogen atoms increases on injection with excess electrons. In contrast, the distance between the next-nearest-neighbor boron atoms decreases for vacancies with boron edges on injection with excess electrons. Our detailed analysis of electronic structures of vacancies unravels the origin of the structural modification of vacancies with regard to their charge state.

DOI: 10.1103/PhysRevB.80.161404 PACS number(s): 61.72.jd, 61.72.uj, 73.20.Hb

I. INTRODUCTION

There has been many theoretical and experimental studies on atomic-scale intrinsic defects in honeycomb networks of C atoms, such as graphene[1–7] and carbon nanotubes.[8–11] Around these defects, a competition between the energetics of the lattice system and the electron system results in rich variations in their electronic and local geometric structures. In regard to monoatomic vacancies, the initial geometry exhibits three dangling bonds involving σ states. However the structure is not stable and so relaxes to form a pentagon and an unpaired σ bond resulting from the pairing of two of three unpaired bonds.[2,3] This relaxation decreases the dangling-bond energy of the electron system, albeit with an increase in stress energy of the lattice system, by reducing the number of unpaired σ electrons on forming the pentagon. In such monoatomic vacancies, it has been reported that the unpaired electron on the σ bond produces a local spin polarization at the defect.[2] By further removing atoms from graphene and nanotubes, we create multiatomic vacancies for which atomic geometry and stability are determined by the delicate and complex balance between the electron and lattice energies; multiatomic vacancies are known to undergo structural relaxation that is characterized by the complex combination of polygons and unpaired σ bonds.[4–7]

In sharp contrast to these atomic vacancies in graphene and carbon nanotubes, little is known of atomic vacancies in hexagonal boron nitride (*h*-BN) of which the network topology is essentially the same as graphene.[12–17] In particular, atomic structure and stability of the multiatomic vacancies has not as yet been addressed. In *h*-BN, the ambivalent nature of covalency and ionicity within the bonding network is an additional factor that determines the atomic structures and energetics of atomic vacancies. This additional factor makes the local environment of vacancies more complex. Recently, transmission electron microscope (TEM) techniques have clearly observed the regular triangle shape of multiatomic vacancies with nitrogen terminated edges.[17] However, the origins of the vacancy shape and the edge atom selectivity are still uncertain.

The purposes of this Rapid Communication are to clarify the various atomic structures and energetics of the multiatomic vacancies in *h*-BN and to give theoretical insight into the vacancy structures observed in the TEM experiment.[17] In this Rapid Communication, we focus on diatomic and tetraatomic vacancies with triangular shape. Our first-principles total-energy calculations show that the energetics of the vacancies strongly depends on the environmental condition such as boron and nitrogen chemical potentials and the electron chemical potential. Furthermore, substantial structural reconstructions are found to take place at the apexes of a multiatomic vacancy. The relaxed atomic structures are qualitatively the same as those in graphene. In addition, we also find that the atomic structures of vacancies depend on their charge state.

II. CALCULATION METHODS

We perform total-energy electronic-structure calculation in the framework of the density-functional theory (DFT).[18,19] The exchange-correlation energy of interacting electrons is treated in terms of the local-density approximation (LDA) with a functional form fitted to the Ceperley-Alder result.[20,21] Norm-conserving pseudopotentials generated by using the Troullier-Martins scheme[22] with the Kleinman-Bylander approximation[23] are adopted to describe the electron-ion interaction. The valence wave functions are expanded in the plane-wave basis set with a cut-off energy of 50 Ry which achieves sufficient convergence for the relative total energies of *h*-BN.[24,25] We adopt the conjugate-gradient minimization scheme for both the electronic-structure calculation and geometry optimization.[26] Structural optimizations are performed iteratively until the remaining force acting on each atom is less than 5 mRy/Å. To simulate the isolated atomic

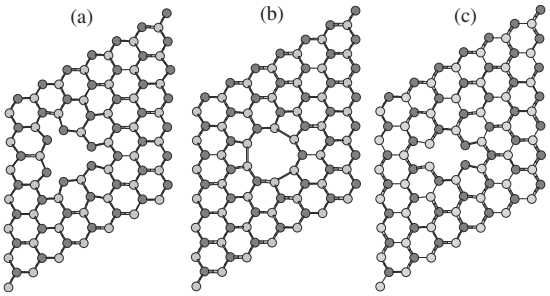

FIG. 1. Optimized structures of (a) the tetra-atomic vacancy with nitrogen-terminated edges V_{B3N1}, (b) the tetra-atomic vacancy boron-terminated edges V_{B1N3}, and (c) the diatomic vacancy V_{B1N1} in *h*-BN. Dark and pale shaded circles denote the nitrogen and boron atoms, respectively.

vacancies in *h*-BN, we use a repeating sheet model with 72 atoms (36 boron and 36 nitrogen atoms) in which each atomic sheet is separated by 9.0 Å to simulate an isolated *h*-BN honeycomb sheet. Integration over the Brillouin zone is carried out using equidistant *k*-point sampling in which the *k*-point density is equivalent to a $576(=24\times24)$ point sampling in the conventional Brillouin zone of a *h*-BN monolayer.

The formation energies of *h*-BN vacancies are calculated as a function of the chemical potentials of atomic species, μ_B and μ_N, and the electron chemical potential or Fermi-level energy μ_e:

$$E_f = E_t - n_N\mu_N - n_B\mu_B + q(\mu_e + \varepsilon_v),$$

where E_t is the total energy and n_N (n_B) is the number of nitrogen (boron) atoms in the supercell. The Fermi-level energy is measured with respect to the energy of the valence-band maximum ε_v. The chemical potentials of boron and nitrogen vary subject to the constraint $\mu_{BN(bulk)}=\mu_B+\mu_N$ in which the upper bounds of the chemical potentials for μ_B and μ_N are limited to those of their bulk phases calculated from the solid nitrogen (α-N_2) and the metallic boron (α-B), respectively.

III. RESULTS AND DISCUSSION

Figures 1(a)–1(c), respectively, show optimized atomic structures of the tetra-atomic vacancy of triangular shape with edges terminated by nitrogen atoms (V_{B3N1}), the tetra-atomic vacancy of triangular shape with edges terminated by boron (V_{B1N3}), and the diatomic vacancy (V_{BN}). In all cases, we find substantial structural relaxation around corners of the vacancies. The relaxations are characterized by strong paring of atoms with twofold coordination situated in the next-nearest-neighbor sites. In V_{BN}, the pairing takes place at both ends of the vacancy by forming B-B and N-N homogeneous bonds. The optimized inter-atomic distances of the B-B and N-N pairs are 1.91 and 1.66 Å, respectively. Similar structural relaxations also take place in tetra-atomic vacancies V_{B3N1} and V_{B1N3}. Here, the pairing is found around the three apexes of the triangular vacancies resulting in the squashed appearance of the triangles. In V_{B1N3}, the distance between the paired boron atoms is 1.95 Å. In contrast, the distance between nitrogen atoms in V_{B3N1} is 1.63 Å.

The strong pairing can be explained in terms of electronic structures of the vacancies. Figures 2(a)–2(c) show the electronic structures and squared wave functions for electronic states associated with V_{B3N1}, V_{B1N3}, and V_{BN}, respectively. It is found that these states exhibit bonding and antibonding natures of σ and π states depending on the paired atom species. In the energy gap between conduction and valence bands, vacancy associated states with bonding and antibonding π states emerge on the B-B pair, while those with antibonding σ state emerge on the N-N pair. These bonding and antibonding states result in strong pairing of atoms situated at the edges of the vacancies.

Figure 3(a) shows the formation energies of vacancies in *h*-BN as a function of the electron chemical potential under nitrogen-rich conditions. Under these conditions, V_{BN} is the

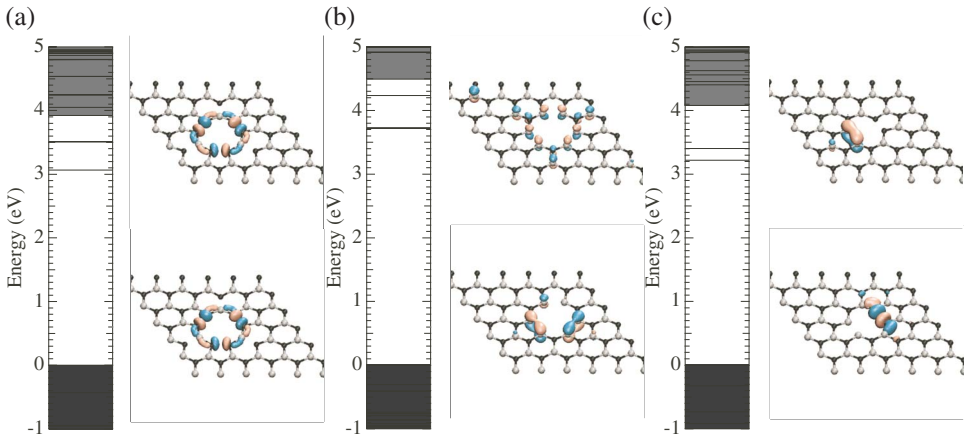

FIG. 2. (Color online) Electronic energy levels of the multiatomic vacancies of (a) V_{B3N1}, (b) V_{B1N3}, and (c) V_{B1N1}. The energies are measured from the top of the valence band. Dark and pale shaded areas denote the electronic states in valence and conduction bands, respectively. Isosurfaces for the squared wave function of the vacancy associated states at Γ point are displayed in the right panel of each figure. Cyan (gray) and pink (light gray) isosurfaces characterize the sign of the wave functions. Dark and pale shaded circles denote the nitrogen and boron atoms, respectively.

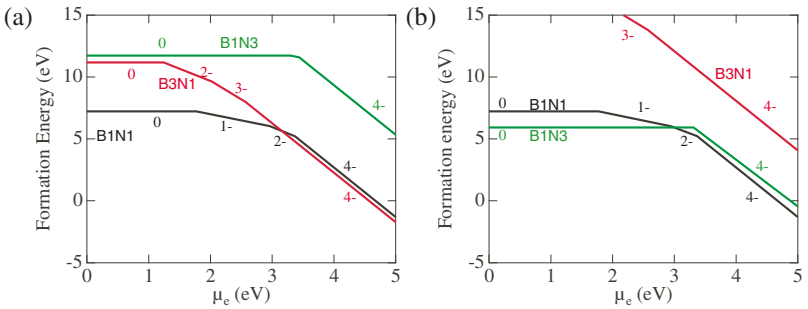

FIG. 3. (Color online) Formation energies (E_f) as a function of Fermi energy μ_e for multiatomic vacancies in h-BN for (a) nitrogen-rich and (b) boron-rich conditions. Green (light gray), red (gray), and black lines denote the energy for V_{B3N1}, V_{B1N3} and V_{B1N1}, respectively. Numbers near lines are the charge states of the corresponding defect.

most stable among the three multiatomic vacancies up to a chemical potential of μ_e=3 eV. Thus, under nitrogen-rich conditions without electron injection, V_{BN} is the favorable structure as in the case of the divacancy in graphene. However, above a chemical potential of 3 eV with negative charge conditions (four excess electrons per cell), the triangular tetra-atomic vacancy with nitrogen terminated edges $V_{B_3N_1}$ is found to be more stable than the divacancy V_{BN}. Thus, the triangular vacancies with nitrogen edges are observed in experiments under electron-rich conditions such as those present in TEM experiments. Indeed, the recent TEM experiment shows triangular vacancies with nitrogen terminated edges.[17] It should be noted that for any electron chemical potential μ_e the triangular vacancy with boron terminated edges are not energetically favorable under nitrogen-rich conditions.

In sharp contrast, under boron-rich conditions, the boron terminated edges are favorable for low electron chemical potential as shown in Fig. 3(b). However, by increasing the electron chemical potential, it is found that the diatomic vacancy with three and four excess electrons is the more stable vacancy structure studied here. In all regions, the triangular vacancy with nitrogen-terminated edges possesses higher formation energy than the other two structures. However, with an increase in the electron chemical potential, the vacancy is substantially stabilized and the energy cost in forming the vacancies is reduced with carrier injection.

Of interest is how the structures of multiatomic vacancies are relaxed under the carrier doping. Figure 4(a) shows an optimized atomic structure of the triangular vacancy V_{B3N1} with nitrogen-terminated edges obtained by injecting four excess electrons per super cell. The shape of V_{B3N1} is found to be considerably modulated by the carrier injection. Nitrogen atoms are shifted in opposite directions from each other restoring their regular triangular shape associated with the vacancy. The distance between the next-nearest-neighbor nitrogen atoms monotonically increases with increasing number of excess electrons; the distances are 2.33 and 2.46 Å for two and four electron doping, respectively. The shape of the vacancy is in agreement with the recent TEM observation on multiatomic vacancies possessing regular triangular shapes with three nitrogen-terminated edges.[17]

The structural reconstruction is ascribed to the electron states associated with the N-N pair in the vacancy. As shown in Fig. 2(b), the levels associated with nitrogen atom pairing exhibit antibonding σ character. Thus, injection of extra electrons increases the interatomic distance of the pair and resumes the original triangular shape of the vacancy. In these cases, the injected electrons are accommodated in unoccupied states of the nitrogen atoms with twofold coordination. Furthermore, the structural modulation induced by electron injection decreases both the lattice and electron energies of the vacancy causing the remarkable stability of the nitrogen-edged vacancy under electron doping.

In sharp contrast, the triangular vacancy with boron-terminated edges V_{B1N3} exhibits opposite characteristics to V_{B3N1}. Figure 4(b) shows an optimized geometry of V_{B1N3} with four excess electrons per cell. The interatomic distance of paired boron atoms is found to be shorter by 0.12 Å than that in V_{B3N1} under neutral charge conditions. In this case, the energy levels associated with the boron atomic pair in the vacancy possess bonding π character. Thus, excess electrons enhance the pairing character of the boron atoms resulting in the remarkable short distance of 1.83 Å. Because of the strong pairing, the vacancy changes in shape to a truncated triangle comprised of threefold coordinated atoms with heterogeneous bonds (B-N bond) and homogeneous bonds (B-B bond).

In regard to the diatomic vacancy, the structural relaxation ascribed to the excess electrons is expected to be a mixture of those in V_{B1N3} and V_{B3N1}. Indeed, the injection of excess electrons increases the N-N distance by occupying the antibonding σ state [Fig. 2(c)]. However, the B-B distance is insensitive to the electron injection. The insensitivity is due to the flexibility of the h-BN network; due to the small number of atoms with twofold coordination, the substantial structural relaxation that decreases the B-B distance is not expect to take place. Furthermore, this insufficient structural relaxation may cause the higher formation energy of the divacancy than that of the triangular vacancy with nitrogen-terminated edges.

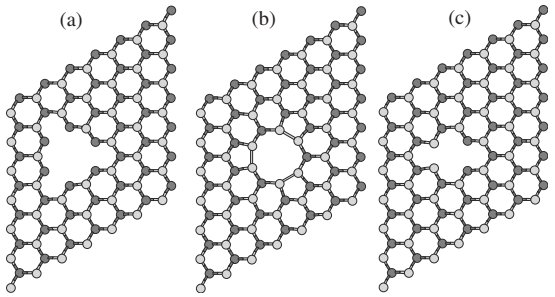

FIG. 4. Optimized structures of multi-atomic vacancies (a) V_{B3N1}, (b) V_{B1N3}, and (c) V_{B1N1} under electron-rich conditions in which four excess electrons are doped into the supercell. Dark and pale shaded circles denote the nitrogen and boron atoms, respectively.

IV. SUMMARY

We have studied the atomic geometry and electronic structure of multiatomic vacancies in hexagonal boron nitride in terms of first-principles total-energy calculations in the density-functional theory. We have shown that the energetics of the vacancies strongly depends on environmental circumstances determined by the concentrations of boron and nitrogen atoms as well as the charge states of the vacancies. It was found that the diatomic vacancy (V_{BN}) is the more favorable vacancy when studied here under nitrogen-rich and neutral conditions. Through doping with excess electrons by increasing the electron chemical potential, the tetra-atomic vacancy with nitrogen-terminated edges possesses lower formation energy than that of the diatomic vacancy. In contrast, under boron-rich conditions, the tetra-atomic vacancy with boron-terminated edges was more favorable up to Fermi energy of 3 eV, while the diatomic vacancy was favorable for higher Fermi energies.

In addition to the energetics, we have also found that the atomic structure of vacancies depended on its charge states. In the tetra-atomic vacancy with nitrogen-terminated edges, the distance between the next-nearest-neighbor nitrogen atoms increased with the injection of excess electrons. Thus, under nitrogen-rich and electron-rich environments, multiatomic vacancies formed regular triangles with nitrogen-terminated edges. The results are in excellent agreement with the recent TEM experiment in which the electrons are intrinsically injected. In contrast, in the vacancy with boron-terminated edges, the distance between the next-nearest-neighbor boron atoms decrease with the injection of excess electrons. Our detailed analysis on the electronic structure of the vacancies has unraveled the origin of the structural modifications of vacancies under various charge states.

ACKNOWLEDGMENTS

We would like to thank A. Oshiyama for providing the DFT program used in this work. This work was partly supported by CREST, Japan Science and Technology Agency, and a Grant-in-Aid for scientific research from the Ministry of Education, Culture, Sports, Science and Technology of Japan. Computations were performed on an NEC SX-8/4B at University of Tsukuba, on an NEC SX-8 at the Yukawa Institute of Theoretical Physics, Kyoto University, and on an NEC SX-9 at the Information Synergy Center, Tohoku University.

[1] A. Hashimoto, K. Suenaga, A. Gloter, K. Urita, and S. Iijima, Nature (London) **430**, 870 (2004).
[2] P. O. Lehtinen, A. S. Foster, Y. Ma, A. V. Krasheninnikov, and R. M. Nieminen, Phys. Rev. Lett. **93**, 187202 (2004).
[3] A. A. El-Barbary, R. H. Telling, C. P. Ewels, M. I. Heggie, and P. R. Briddon, Phys. Rev. B **68**, 144107 (2003).
[4] Z. Tang, M. Hasegawa, T. Shimamura, Y. Nagai, T. Chiba, Y. Kawazoe, M. Takenaka, E. Kuramoto, and T. Iwata, Phys. Rev. Lett. **82**, 2532 (1999).
[5] J. M. Carlsson and M. Scheffler, Phys. Rev. Lett. **96**, 046806 (2006).
[6] K. Yamashita, M. Saito, and T. Oda, Jpn. J. Appl. Phys. **45**, 6534 (2006).
[7] M. Saito, K. Yamashita, and T. Oda, Jpn. J. Appl. Phys. **46**, L1185 (2007).
[8] Y. Ma, P. O. Lehtinen, A. S. Foster, and R. M. Nieminen, New J. Phys. **6**, 68 (2004).
[9] M. Igami, T. Nakanishi, and T. Ando, J. Phys. Soc. Jpn. **68**, 716 (1999).
[10] S. Lee, G. Kim, H. Kim, B.-Y. Choi, J. Lee, B. W. Jeong, J. Ihm, Y. Kuk, and S.-J. Kahng, Phys. Rev. Lett. **95**, 166402 (2005).
[11] A. V. Krasheninnikov, K. Nordlund, M. Sirvio, E. Salonen, and J. Keinonen, Phys. Rev. B **63**, 245405 (2001).
[12] R.-F. Liu and C. Cheng, Phys. Rev. B **76**, 014405 (2007).
[13] W. Orellana and H. Chacham, Phys. Rev. B **63**, 125205 (2001).
[14] L. Museur, E. Feldbach, and A. Kanaev, Phys. Rev. B **78**, 155204 (2008).
[15] G. Y. Gou, B. C. Pan, and L. Shi, J. Phys. Chem. C **112**, 19353 (2008).
[16] A. Zobelli, C. P. Ewels, A. Gloter, G. Seifert, O. Stephan, S. Csillag, and C. Colliex, Nano Lett. **6**, 1955 (2006).
[17] C. Jin, F. Lin, K. Suenaga, and S. Iijima, Phys. Rev. Lett. **102**, 195505 (2009).
[18] P. Hohenberg and W. Kohn, Phys. Rev. **136**, B864 (1964).
[19] W. Kohn and L. J. Sham, Phys. Rev. **140**, A1133 (1965).
[20] J. P. Perdew and A. Zunger, Phys. Rev. B **23**, 5048 (1981).
[21] D. M. Ceperley and B. J. Alder, Phys. Rev. Lett. **45**, 566 (1980).
[22] N. Troullier and J. L. Martins, Phys. Rev. B **43**, 1993 (1991).
[23] L. Kleinman and D. M. Bylander, Phys. Rev. Lett. **48**, 1425 (1982).
[24] S. Okada and A. Oshiyama, Phys. Rev. Lett. **87**, 146803 (2001).
[25] S. Okada, S. Saito, and A. Oshiyama, Phys. Rev. B **65**, 165410 (2002).
[26] O. Sugino and A. Oshiyama, Phys. Rev. Lett. **68**, 1858 (1992).